energies

MDPI

Article

New Method of Degradation Process Identification for Reliability-Centered Maintenance of Energy Equipment

Konstantin Zadiran * and Maxim Shcherbakov *

Computer Aided Design Department, Volgograd State Technical University, 400005 Volgograd, Russia
* Correspondence: konstantin.zadiran@gmail.com (K.Z.); maxim.shcherbakov@vstu.ru (M.S.)

Abstract: Advancements in energy technologies created a new application for gas turbine generators, which are used to balance load. This usage also brought new challenges for maintenance because of harsh operating conditions that make turbines more susceptible to random failures. At the same time, reliability requirements for energy equipment are high. Reliability-centered maintenance based on forecasting the remaining useful life (RUL) of energy equipment, offers improvements to maintenance scheduling. It requires accurate forecasting methods to be effective. Defining stages in energy equipment operation allows for the improvement of quality of data used for training. At least two stages can be defined: normal operation and degradation process. A new method named Head move—Head move is proposed to robustly identify the degradation process by detecting its starting point. The method is based on two partially overlapping sliding windows moving from the start of operation to the end of life of the energy equipment and Kruskal-Wallis test to compare data within these windows. Using this data separation, a convolutional neural network-based forecasting model is applied for RUL prediction. The results demonstrate that the proposed degradation process identification (DPI) method doubles the accuracy when compared to the same forecasting model but without degradation process identification.

Keywords: energy equipment; gas turbines; reliability-centered maintenance; remaining useful life; degradation process identification; deep neural networks; Kruskal-Wallis test

Citation: Zadiran, K.; Shcherbakov, M. New Method of Degradation Process Identification for Reliability-Centered Maintenance of Energy Equipment. *Energies* **2023**, *16*, 575. https://doi.org/10.3390/en16020575

Academic Editors: Alla Kravets, Valery Meshaklin, Petros Groumpos and Chirag Bhimani

Received: 15 December 2022
Revised: 26 December 2022
Accepted: 29 December 2022
Published: 4 January 2023

1. Introduction

Gas turbines are used for various applications from energy generation to propulsion, gas compression, etc. With the shift towards clean energy production, a new use for gas turbines as a supporting back-up load balancing tool has emerged [1]. Gas turbines have advantages of small footprint, high power to weight ratio, mobility and quick startups as well as mobility and fast deployment [2,3].

This use also brought new challenges which include a variety of operating conditions, frequent and irregular operation cycles [2,4]. These make gas turbines more susceptible to failures, which are mostly random [5]. Likewise, latest technologies which allow making turbines more efficient make them more complex as well, which complicates diagnostics making it more costly as well [6]. With that, the described case requires high availability and readiness [7].

The failures cause downtime by making gas turbine unavailable for energy production and require costly repairs and even replacement of a unit altogether [6]. Failures in total may account for up to a third of the operating cost [8]. These factors require new improved flexible and robust strategies for the maintenance of energy generating equipment.

There are multiple strategies to conduct maintenance. All of them can be divided into two groups: reactive and proactive strategies [9]. The reactive or run-to-failure strategy is to perform maintenance in the event of a failure. This is used mostly for inexpensive, expendable or non-serviceable equipment. In general, only proactive strategies are used for the maintenance of complex energy equipment. These include periodic and preventive strategies, which are used either exclusively or in conjunction with each other [10].

Periodic strategy is the most prevalent form of maintenance nowadays. Periodic maintenance is a regularly scheduled operation based on operating time, generally specified in manufacturer recommendations. While this strategy is easy to implement and follow, it does not prevent random failures, which constitute more than three quarters of all failures [6] and might lead to an increased probability of failure right after maintenance. It also might not be adequate for harsh and extreme operating conditions, where equipment wear is greater than in average conditions.

Preventive maintenance is based on the inspection of condition of energy equipment using non-destructive monitoring methods. This strategy uses predetermined acceptable ranges for values of parameters [11]. Repairs may be scheduled if the inspection of parameters or condition of energy equipment shows out-of-range deviation in readings or other flaws in operation, such as excessive noise or vibration.

Industry 4.0 brought new digital technologies, as IoT (internet of things), cloud computing and big data to enable improved failure detection and optimized asset management through the use of computerized analytics and machine learning [12]. Advancements in IoT (internet of things) allowed better availability of sensors, improvements to data transfer and storage [13].

More advanced and promising maintenance strategy that originates from concept of Industry 4.0 is a proactive reliability-centered maintenance, which is based on forecasting of health index and remaining useful life of the energy equipment [10]. This is a data-driven strategy that relies on data collected from the sensors to make forecasts about future condition of energy equipment and possible failures. Having such forecast may allow the decision-maker to adjust maintenance schedule or to perform additional inspections.

The main parameter for this strategy is the remaining useful life (RUL) [14]. It is defined as operating time between current or set moment in time t_{now} and the time of the end of life of energy equipment t_{EOL} as Formula (1) shows.

$$RUL = t_{EOL} - t_{now} \tag{1}$$

Figure 1 demonstrates RUL, health index and the relation between them. The end of life might be either the next failure of energy equipment or a state when further operation is impossible without a major loss of functionality or is going to lead to a failure.

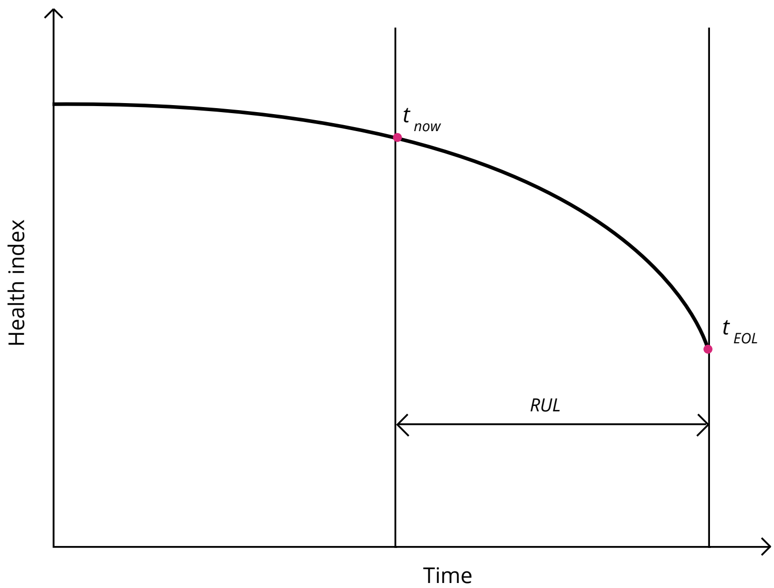

Figure 1. Remaining useful life illustration (adapted from [14]) .

The hypothesis of this paper is that if the accuracy of defining stages of energy equipment operation and splitting data according to them is improved, forecasting RUL is going to become more accurate. The contribution of the paper is a new proposed method for degradation process identification (DPI) as a part of reliability-centered maintenance methodology. The idea if the method is based on sliding windows and Kruskal-Wallis test to compare data within these windows. A Head Move—Head Move strategy of sliding windows allows to define starting point of energy equipment degradation. A method uses two partially overlapping sliding windows moving from start of operation to the end of life of energy equipment. Based on this data separation, we applied a convolutional neural network-based forecasting model for RUL prediction.

2. A Method of Degradation Process Identification as a Part of Reliability-Centered Maintenance Methodology

2.1. Reliability-Centered Maintenance Methodology

Methodology of a typical reliability-centered maintenance that implements RUL-based predictive maintenance for energy equipment consists of the following steps [15,16]: data acquisition (DAcq), data pre-processing (DPP), data analysis (DAn), decision support (DS), maintenance implementation(MI) and operation (Op). Figure 2 illustrates the aforementioned methodology. Highlighted in red is a focus of this article.

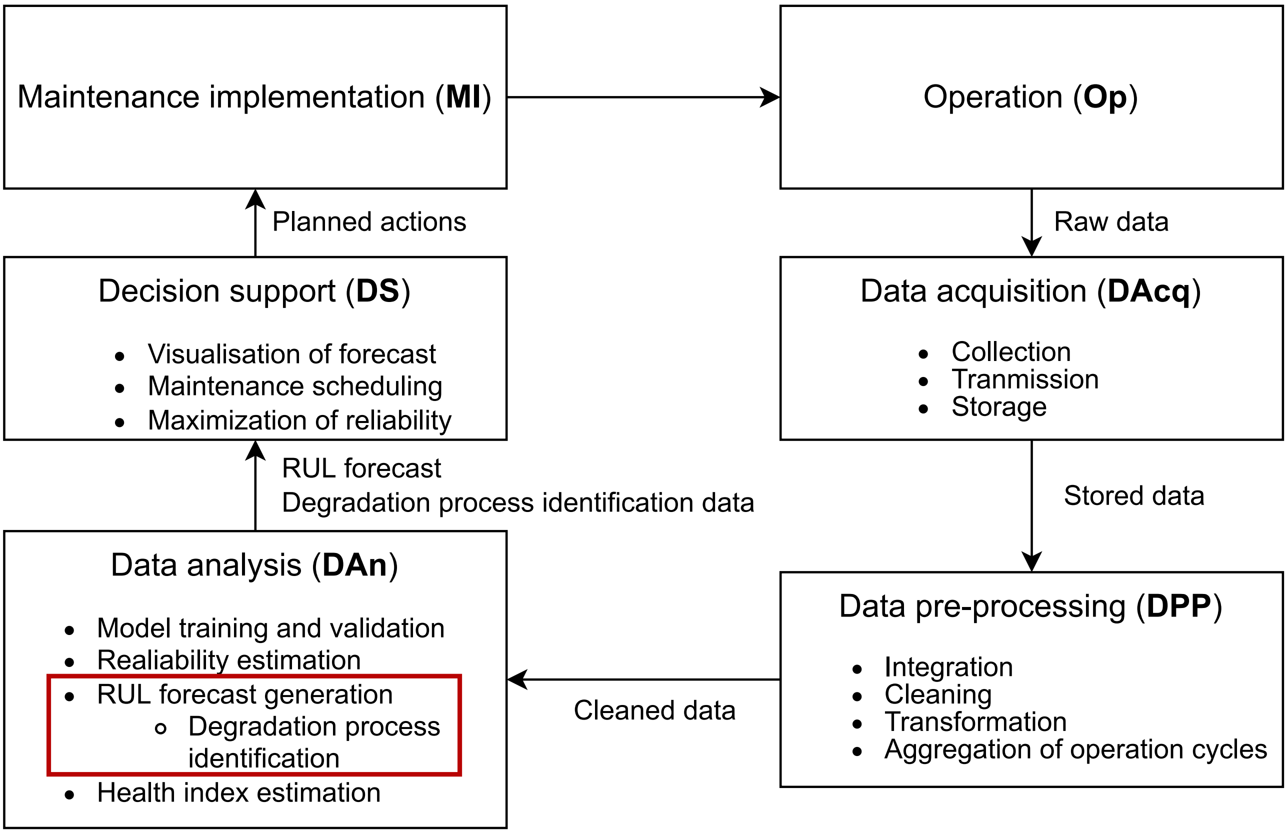

Figure 2. Flowchart of the entire predictive maintenance methodology (adapted from [15,17]).

DAcq is the first step of process, where data are collected from equipment through a network of sensors to a centralized storage. At the DPP step, the data are integrated, cleaned, transformed. Data for operation cycles is aggregated to a single value for each parameter of energy equipment [18]. During DAn, the step data analysis and machine learning are used to generate a RUL forecast.

At stage of DS maintenance schedule is adjusted according to the forecast, as displayed at Figure 3. The maintenance is scheduled for t_{MI} at a t_{now} moment in time when the failure is forecasted to occur at t_{EOL}. This leads to the MI step, at which the schedule from the previous step is implemented in a real world at t_{MI} for improved energy equipment operation.

Managerial actions that are planned at the DS step are significantly affected by the accuracy of RUL forecast, produced at DAn step—the higher the accuracy of the forecast, the more efficient actions can be planned and carried out at MI step [14]. Managerial actions might be such as the equipment's mode optimizing, risk-based inspection, repair, and many others.

Proposed DPI method is a part of DAn step, which is expressed in mitigation of inaccuracies of RUL forecasting through splitting data into two stages—the normal mode of operation and degradation process, which is conducted before model training. For testing purposes, the whole method includes the DPP step as well, consisting of data splitting, transformation, normalization, and other parts of DAn step, including CNN-based model, its training and validation, and the generation of the forecast.

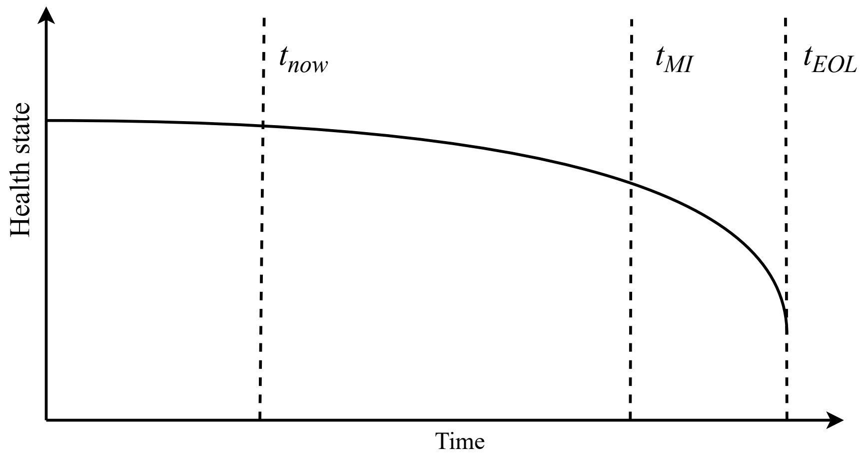

Figure 3. Maintenance scheduling at DS step (adapted from [17]).

2.2. An Overview of State-of-the-Art Research of RUL Forecasting

The accuracy of RUL forecast is a crucial aspect of the efficient application of the proactive strategy [14]. The more accurate the forecast is, the more precision is available for maintenance scheduling, which means that it would not be scheduled too early or too late. This, in turn, leads to a more optimal number of stops for maintenance and lower downtime in general.

There are many RUL prediction methods and strategies based on a wide range of forecasting algorithms and models. In the review [19], L. Zhang et al. looked at RUL forecasting methods, based on SVM-based algorithms and their advantages for multivariate time series analysis. C. Lu et al. investigated [20] stacked denoising autoencoder (SDA)—a deep learning method, which was shown to be suitable for certain health state identifications for signals containing ambient noise and working condition fluctuations for effective fault diagnostics. H. Z. Huang et al. reviewed [21] Support vector machine (SVM)-based methods and pointed out the ability to continually improve SVM and obtain a novel idea for RUL prediction using SVM in future works, particularly with tracking of the degradation process. G. A. Susto et al. presented [9] a multiple classifier machine learning methodology for predictive maintenance. Methodology included training multiple classification modules with different prediction horizons to provide different performance tradeoffs in terms of frequency of unexpected failures and unexploited lifetime, and then employing this information in an operating cost-based maintenance decision system to minimize the expected costs. P. G. Nieto et al. presented [22] a hybrid PSO–SVM-based model for the prediction of the remaining useful life of aircraft engines. The proposed hybrid model combined the support vector machines with the particle swarm optimization (PSO) technique. M. Yan et al. presented [23], a method of RUL prediction of bearings, which can evaluate the degradation stage of bearings through dimensionless measurements and exploit the optimal RUL prediction through hybrid degradation tracing model in the degradation stage, which is based on an SVM classificator. T. Praveenkumar et al. investigated [24], the usage of SVM-based models and time domain statistical features, such as mean, median, etc., to forecast failures in gearboxes. K. Dhalmahapatra et al. developed [25] a decision support system for failure forecasting, using a multi-step knowledge discovery process involving multiple correspondence analysis (MCA), t-SNE algorithm and K-means clustering. S. S. Ng et al. proposed [26] a naive Bayes model for RUL prediction of batteries under different operating conditions and showed its competitiveness in accuracy with SVM based models and importance of different operating conditions and their impact on degradation of equipment. S. Patil et al. proposed a new approach for RUL prediction [27], which includes the use of ensemble regression techniques such as Random Forest and Gradient Boosting for prediction of RUL with time-domain features, which are extracted from the given data.

Artificial neural networks are common in recent years. There are several main directions, focusing on different architectures, such as LSTM and CNN.

J. Deutsch et al. [28] presented a deep belief network-based approach for RUL prediction of rotating components for big data applications. P. Khumprom et al. [29] developed a new model, based on recurrent neural networks with amplified dropout to increase number of training runs. R. Zhao et al. [30] investigated application of Long Short-Term Memory networks (LSTMs) for machine health monitoring in the first study about a empirical evaluation of LSTMs-based machine health monitoring systems and introduced a real life tool wear test. A. Sagheer and M. Kotb proposed [31] a pre-trained LSTM-based stacked autoencoder (LSTM-SAE) approach in an unsupervised learning fashion to replace the random weight initialization strategy adopted in deep LSTM recurrent networks to improve the performance in modelling multivariate time series (MTS) data, particularly when attempting to process highly non-linear and long-interval MTS datasets. Y. Zhang et al. [32] proposed an adaptive recurrent neural network (RNN) to predict the remaining life of Li batteries, and a technique for optimizing the weights of the network structure through a cyclic Levenberg–Marquardt method. F. Zhou et al. [33] proposed an early diagnosis method based on Deep neural networks (DNN). The high-dimensional fault features extracted by deep learning are reduced into one-dimensional, and then the life prediction model is constructed by using the nonlinear fitting method. L. Mao et al. [34] developed a hybrid LSTM-STW and GS-LM method to decompose the data into high-frequency and low-frequency components, create separate RUL predictions using the LSTM-based model and integrate them to obtain final prediction. B. Long et al. [35] proposed LSTM-based forecasting method with an improved data construction method for a lower number of data samples available, which is able to increase the accuracy of forecast for lithium-ion batteries.

G. S. Babu et al. [36] made the first application of deep convolutional neural networks (CNN) to RUL forecasting. K. B. Lee et al. [37] introduced the FDC-CNN model, based on CNN architecture, in which a receptive field tailored to multivariate sensor signals slides along the time axis, to extract fault features, which enables the association of the output of the first convolutional layer with the structural meaning of the raw data, making it possible to locate the variable and time information that represents process faults. L. Ren et al. [38] proposed new feature extraction method to obtain the eigenvector that is suitable for deep CNN. In the prediction phase, a smoothing method is proposed to deal with the discontinuity problem found in the prediction results. J. Zhao et al. [39] reviewed forecasting methods for RUL and outlined the suitability of CNN for monitoring massive data and its ability to realize automatic feature extraction and recognition without manual participation and intervention. C. Sai et al. proposed [14,40] a new hybrid approach for RUL forecasting introducing a model, based on combination of CNN and LSTM and showed accuracy improvements of a combined approach compared to only using the CNN or LSTM-based models.

Several articles [14,20,22] cover the forecasting of turbofan engines [18], which is the main focus of this article. Out of them, methods based on convolutional neural networks (CNN) are looking to be the most promising, being widely accepted and very precise, and reaching an accuracy of 18.90 (RMSE) [14].

However, as much as we upgrade architecture of forecasting methods, at some point they going to reach a limit of performance. After that, optimizations and improvements for forecasting procedure that can be performed beyond the scope of forecasting model itself are going to play an important role in increasing accuracy.

Research [23,41] shows the viability of splitting data into separate parts or modes of operation in accordance to the health index of energy equipment for improving accuracy of forecast. Basically, at least two modes of operation can be distinguished: normal operation and degradation [41] and a separate forecasting models can be built for each of the parts. For these parts, the task of splitting is essentially a task of finding a point in time series at which the degradation starts.

2.3. An Idea of the DPI Method

During the operation of energy equipment, after some point in time, the degradation process begins. An example of operation data is provided at Figure 4. Figure 5 shows an illustration of the degradation process.

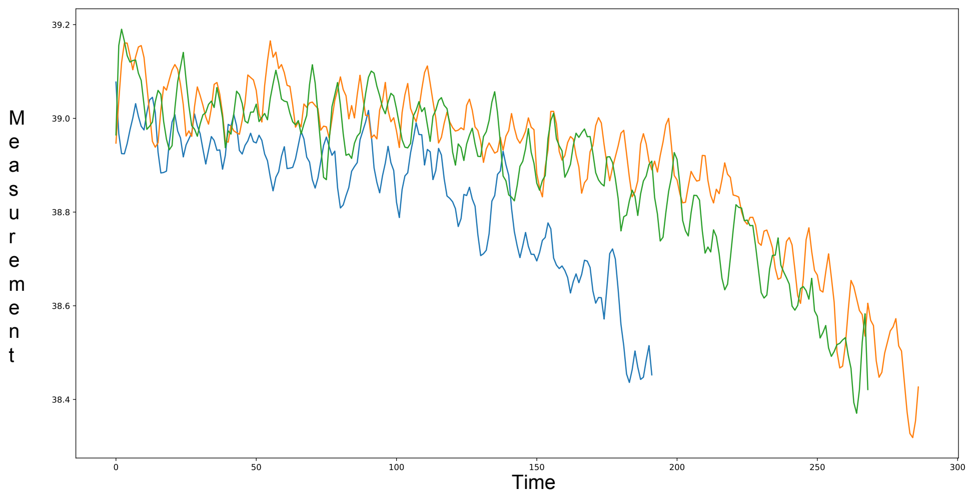

Figure 4. Example of data of operation of energy equipment [18] with values of three arbitrary sensors over time.

To determine the point at which the degradation process begins t_{degr} (starting point of degradation) we propose a new DPI method based on sliding windows. We apply two windows w_1, w_2 of size w to a univariate time series and compare data values in these windows.

There are two types of windows possible in our framework: *head* and *tail*. *Head* is a window that has its initial position at the beginning of the operation. *Tail* is a window that originates at the end of useful life.

We consider two possible operations for manipulating the position of windows: *move* and fix. *Move* is an operation which changes the position of window against time series. It has two parameters: distance and direction. Distance is measured in number of consecutive measurements on which position is changing. In the proposed method, the distance is set to 1 for every case.

Which direction the window in is moving is dependent on its type. Direction can be either forward, which means from beginning of operation to end of life, and backwards, which is the opposite. *Head* is moved in a forward direction, *tail*—in backward direction. Fix is an operation that puts the window at a certain preset position and does not move it over time.

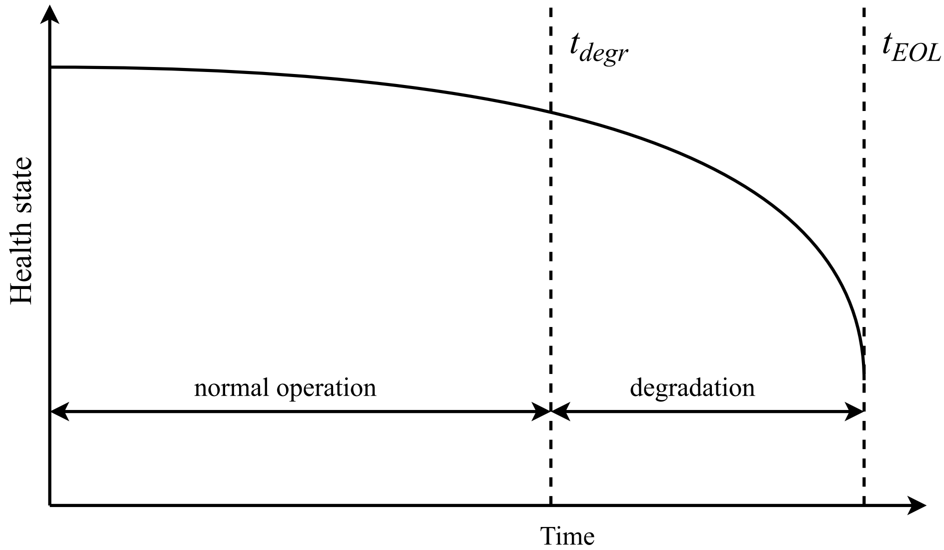

Figure 5. Degradation process visualization (adapted from [41]).

To compare data within windows we use the Kruskal-Wallis test [42]. We assume that windows are different if the null-hypothesis is failed for two given windows, otherwise they are similar. Windows which belong to the normal operation stage are expected to be similar to each other and windows which belong to degradation stage are different. This is because during normal operation the sensor data stay relatively unchanged, and during the degradation stage we observe significant changes in the data.

Positive check and negative check are the terms used for the description of the comparison results. A positive check is a result of the comparison of two windows with the Kruskal-Wallis test, which returns the σ value of more than 0.05, which means that windows can be considered similar. A negative check is a result of comparison of two windows with Kruskal-Wallis test, which returns the σ value of less than 0.05, which means that windows cannot be considered similar.

In this framework, we distinguish five possible strategies of moving windows. They are provided in Table 1. Other possible strategies are either duplicates of the provided ones or not suitable for time series analysis (e.g., two fixed windows).

Table 1. Window moving strategies.

Strategy	First Window Type	First Window Operation	Second Window Type	Second Window Operation
HMTF	Head	Move	Tail	Fix
HMTM	Head	Move	Tail	Move
HFTM	Head	Fix	Tail	Move
HFHM	Head	Fix	Head	Move
HMHM	Head	Move	Head	Move

HMTF strategy allows for comparing every part of the historical data to the final range just before the end of life by moving window w_1 towards t_{EOL} where w_2 is located. This is beneficial because we can safely assume that the process near the end of life is in the degradation stage. However, this strategy has a disadvantage of being able to be used only on historical data and not on real-time data, because it requires the t_{EOL} value to work. Moreover, it has a requirement for comparison operation, where the check for two windows in the degradation stage needs to be positive. With our selected method of comparison, it is not possible due to the fact that windows in the degradation stage are different. Figure 6 illustrates the idea of the HMTF strategy.

The blue line at the Figures 6–10 is an example of the RUL forecast obtained using the framework [43] for the data [18].

The HMTM strategy consists of the two windows w_1 and w_2 moving towards each other. At the start, two windows are assumed to be different, because they should belong to different processes. The beginning of the degradation stage is determined when the check for data in the windows is positive. This strategy also has a disadvantage of requiring a value of t_{EOL} to function; hence, it can be only used on historical data. Demonstration of HMTM is provided at Figure 7 and shows how the proposed method works for the HMTM strategy.

The HFTM strategy is based on the following: a window w_1 is fixed at beginning of operation and a window w_2 is moving from the end of life towards the first one. We assume that data at the beginning of the operation belongs to a normal operation stage. At the start, a comparison of data belonging to windows should return a negative check result. The beginning of degradation is at the point where the check result becomes positive. This strategy also has a disadvantage of requiring the position of the end of life point t_{EOL} to function; hence, it can be only used on historical data. The demonstration of HFTM strategy is provided at Figure 8.

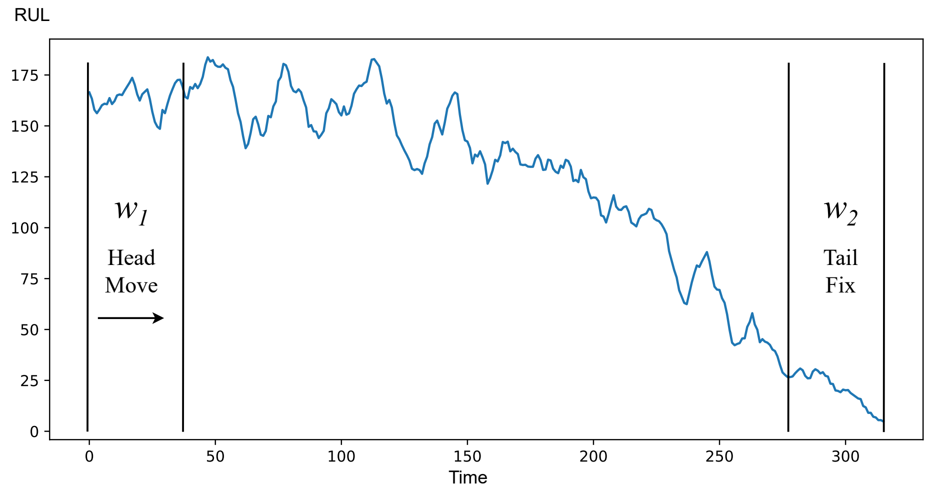

Figure 6. Explanation of HMTF strategy. We observe that one sliding window of observation from head is moving while the sliding window from tail is fixed.

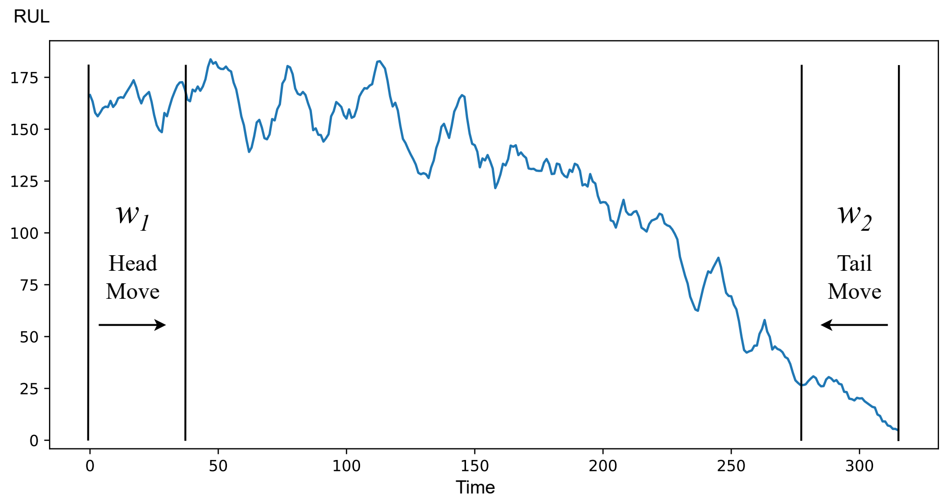

Figure 7. Explanation of HMTM strategy. We see both sliding windows of observation from head and tail are moving towards each other.

HFHM strategy consists of the w_1 window fixed at the beginning of the operation and other window w_2 moving from the first one towards end of life. At the start, the windows should be similar. The beginning of degradation is at the point where they become different. This strategy is similar to HFTM and is an improvement on it, because it does not require it to know the value of t_{EOL}. An illustration of of HFHM is provided at Figure 9.

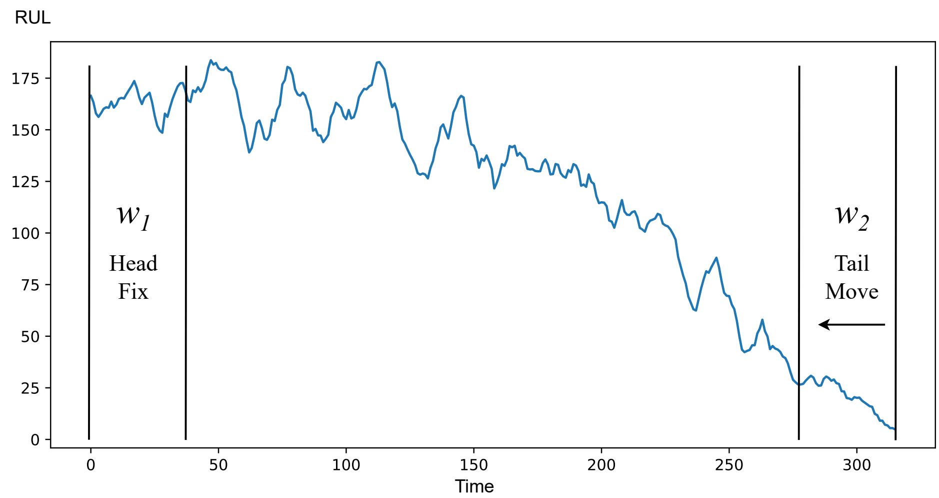

Figure 8. Explanation of HFTM strategy. We see one sliding window of observation from tail is moving while the sliding window from head is fixed.

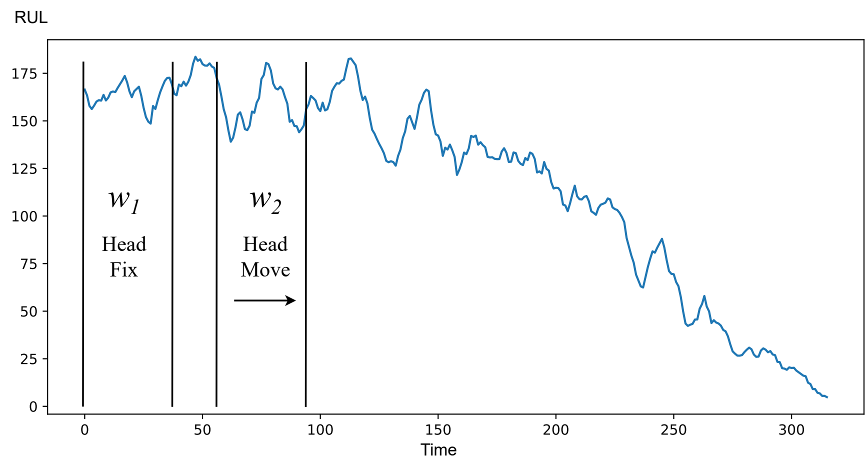

Figure 9. Explanation of HFHM strategy. We see one sliding window of observation from head is moving while the other window at the head of observation is fixed.

HMHM strategy consists of two windows w_1, w_2 moving from the beginning of the operation towards the end of life. The distance and amount of overlap of two windows is described by parameter lag, which is a difference between the starting points of windows, as shown in Formula (2).

$$lag = t_{w_2} - t_{w_1}, \tag{2}$$

where t_{w_1}, t_{w_2} are the positions of the left edges of windows w_1 and w_2, accordingly.

If $lag < w$ then two windows are overlapping.

The beginning of degradation is at the point where w_1, w_2 cannot be considered similar, i.e., Kruskal-Wallis value of $\sigma < 0.05$. Demonstration of HMHM is provided at Figure 10.

This strategy is more robust than the HFHM, because it accounts for possible drift in values during normal operation, which otherwise might have been considered as a sign of degradation. To achieve this, the strategy utilizes a lag of a second order l_2 parameter to adjust the sensitivity of detection. The meaning of this parameter is a number of consequent negative checks. The higher the value of the parameter, the less sensitive this strategy is for data fluctuations, and vice-versa—the lower the value of the parameter, the more sensitive is the strategy.

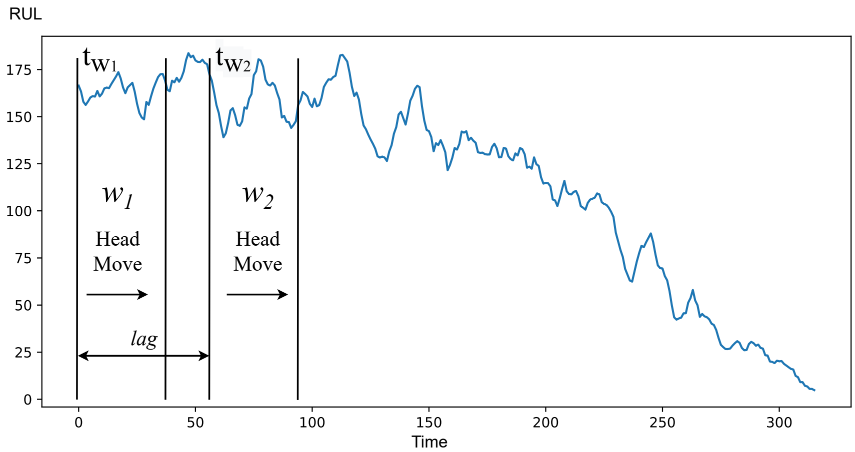

Figure 10. Explanation of HMHM strategy. We see both sliding windows of observation from head are moving with a defined lag.

2.4. A Scheme of the DPI Method

The general description of the DPI method is depicted at the Figure 11. Algorithm 1 shows operation of the method for HMHM strategy to produce the degradation start point t_{degr} on data x using two moving windows w_1 and w_2 with the size w. HMHM strategy also requires lag l input parameter, which is the distance between two windows w_1 and w_2. Another parameter is l_2, which is a lag of a second order, i.e., the number of iterations for which Kruskal-Wallis condition has to be met in order to consider it a true start of the degradation process and reduce noise.

Algorithm 1 Determining degradation start point using HMHM strategy.

Input: $x, w > 0, t_0 = 0, t_{EOL} > 0, l > 0, l_2 \geq 0$
Output: t_{degr}
  $t_{w_1} \leftarrow 0$ ▷ Initial position of the first window
  $t_{w_2} \leftarrow 0$ ▷ Initial position of the second window
  $PointFound \leftarrow false$ ▷ Flag that indicates whether degradation start point was found
  $l_2^{curr} \leftarrow 0$ ▷ Current number of consequent negative checks
  while $PointFound \neq true$ **do**
    if $t_{w_2} + w + l \leq t_{EOL}$ **then** ▷ Reached end of data without finding point
      $t_{degr} \leftarrow 0$
      $PointFound \leftarrow true$
    else
      $d_1 \leftarrow x[t_{w_1}; t_{w_1} + w]$ ▷ Data in the first window
      $d_2 \leftarrow x[t_{w_2}; t_{w_2} + w]$ ▷ Data in the second window
      $\sigma \leftarrow CalculateKruskalWallis(d_1, d_2)$ ▷ Calculate σ using Kruskal-Wallis test
      if $\sigma \leq 0.05$ **then**
        $l_2^{curr} \leftarrow l_2^{curr} + 1$
      else
        $l_2^{curr} \leftarrow 0$
      end if
      if $l_2^{curr} = l_2$ **then**
        $t_{degr} \leftarrow t_{w_1}$
        $PointFound \leftarrow true$
      else
        $t_{w_1} \leftarrow t_{w_1} + 1$ ▷ Move windows a step forward and repeat
        $t_{w_2} \leftarrow t_{w_2} + 1$
      end if
    end if
  end while

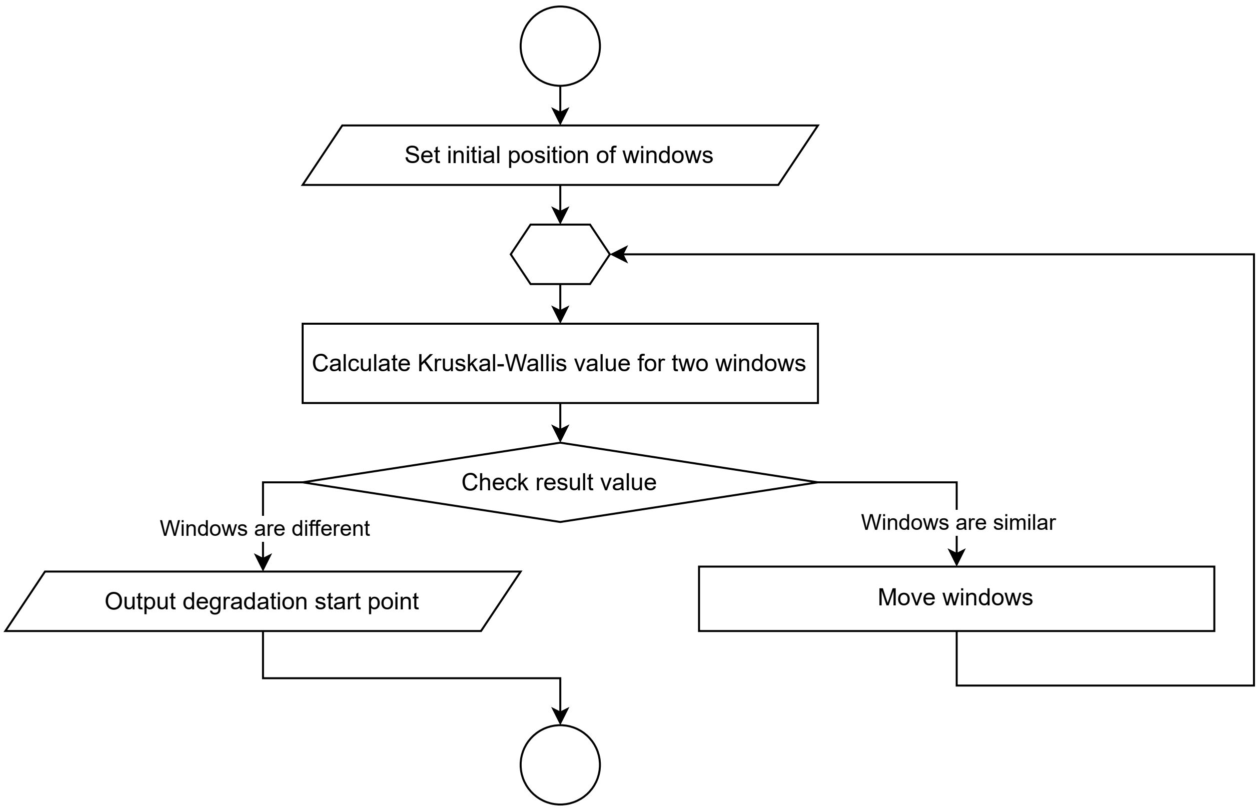

Figure 11. Proposed method for determination of degradation start point.

2.5. Update RUL Forecasting Using Proposed Method

To mitigate inaccuracies of RUL forecasting in models that use the whole data from the beginning of the operation to the end of life, we split data into two stages—normal mode of operation and the degradation process. To do this, we used a DPI method described in Section 2.3. Figure 12 displays the top level diagram of the whole implementation of the method for RUL forecasting.

At step 1 of the method, the raw historical data is loaded from .csv file. The data consists of the following attributes: engine number, cycle number, parameters and values from various sensors.

At step 2, the data are prepared for further use in training forecasting models. First, the remaining useful life (RUL) is calculated for each line. Then, all parameters with zero variation are removed from the data. Then, all input parameters and sensor values are normalized. Finally, inputs and outputs for learning are prepared. The RUL value of measurement is taken as an output. The two-dimensional array of sensor parameters of length w, that represents w consequent measurements before the corresponding RUL value, is formed as input.

At step 3, the data are split into two parts: p_1 of size 20 percent and p_2 of 80 percent of total data.

At step 4, data for the degradation process are split. Figure 13 provides a flowchart with a further breakdown of this step. At step 4.1, part of the data p_1 of size 20 percent is read. At step 4.2, this p_1 data are used for training the first CNN-based forecasting model. At step 4.3, the trained model is used to forecast the RUL for p_2 data.

Then, at step 4.4, points at which the degradation begins are determined. Figure 11 provides a flowchart of the determination of degradation start point. At step 4.4.1, the initial positions for moving windows are set according to the selected strategy. At step 4.4.2, the statistical test is performed on data that these windows cover. At step 4.4.3, the test result check is performed. At step 4.4.4, if the windows are different, the degradation start point is set at the location of one of the windows. At step 4.4.5, if the windows are the same, their positions are moved and the execution moves to step 4.4.2.

At step 4.5, data are split into normal process and degradation, where the degradation data are located after the degradation start point. At step 4.6, these data are outputted for further use in the following steps.

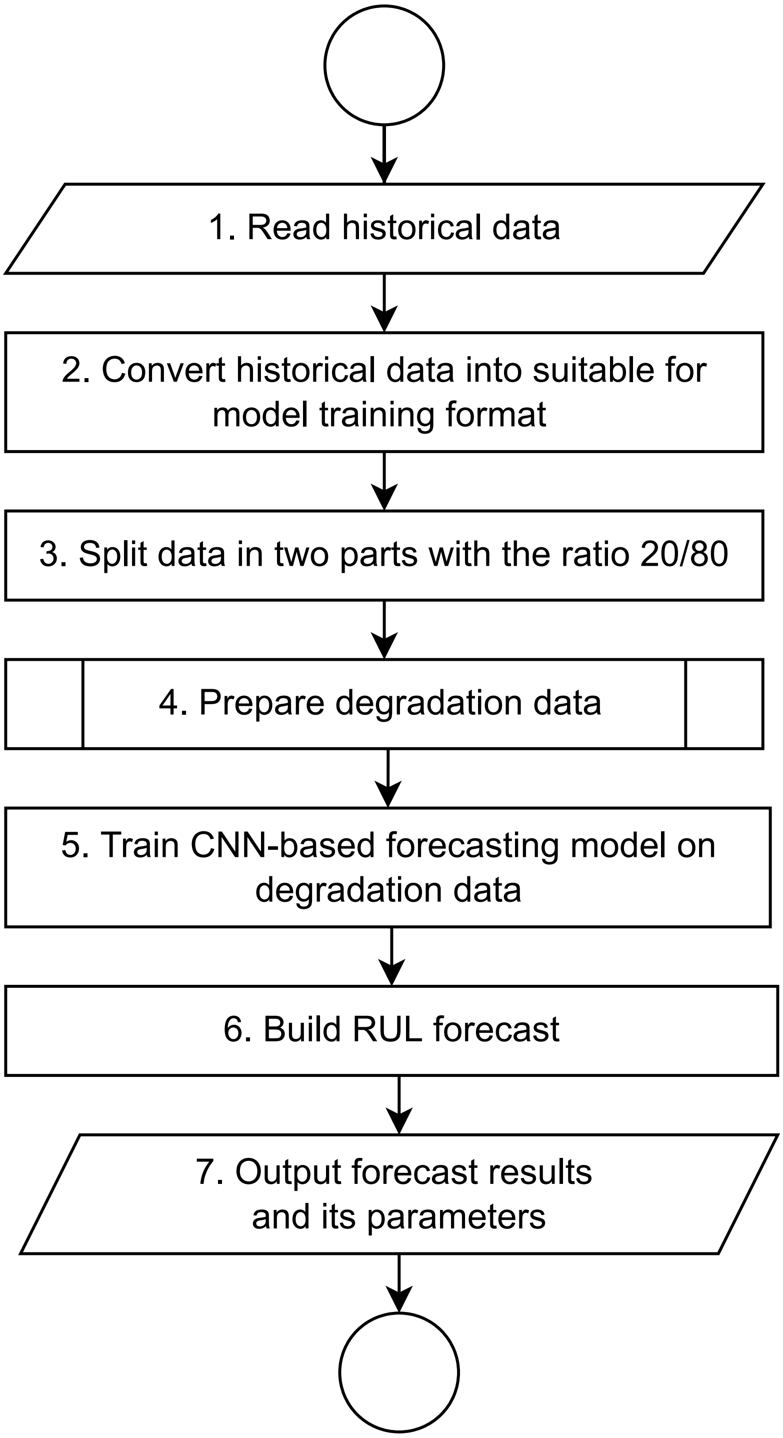

Figure 12. Proposed RUL forecasting method with DPI.

At step 5, data from step 4 are used for training the CNN-based forecasting model. At step 6, the forecast for RUL is built using model from step 5. At step 7, the forecast result is outputted.

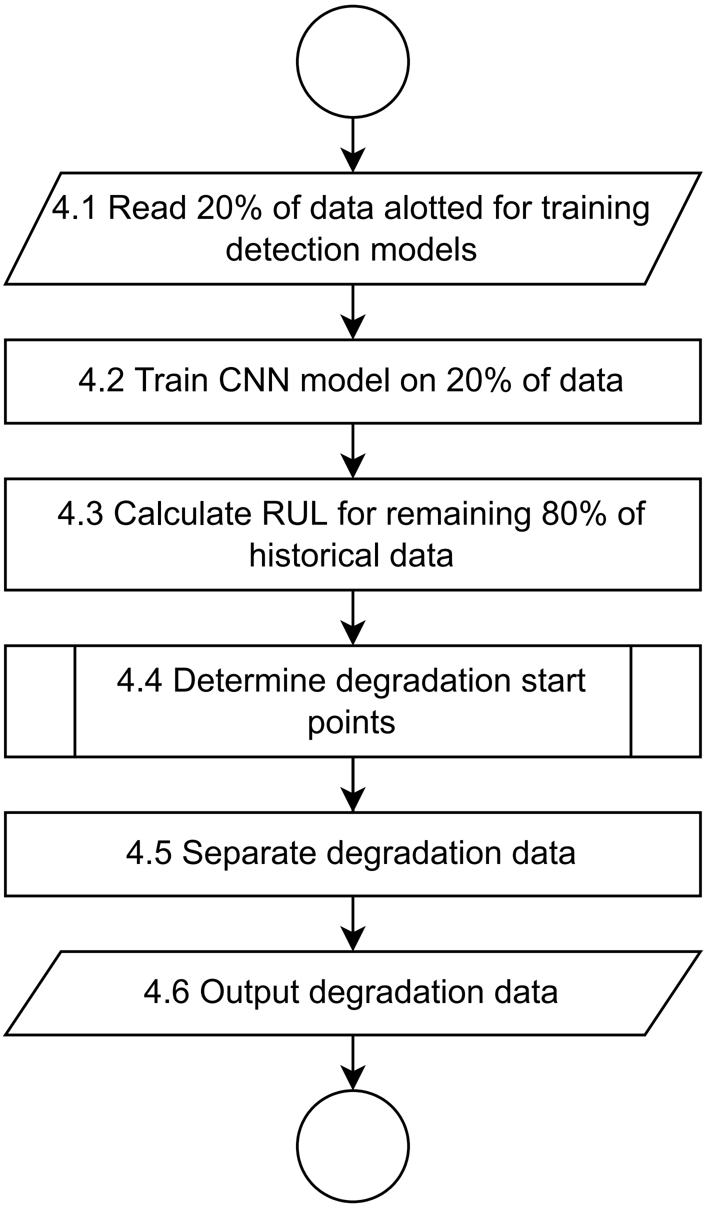

Figure 13. Proposed method for preparation of degradation data.

2.6. CNN Architecture

We use the convolutional neural network (CNN) as a benchmark method as well as in conjunction with proposed methods' strategies. CNN is a Deep Learning algorithm, which can take in an input two-dimensional array, assign importance (learnable weights and biases) to various aspects/objects in the image and be able to differentiate one from the other [44]. Figure 14 provides a visual scheme of the CNN used in the experiment.

The specific model that we use in this research was developed by Cuong Sai [14]. Figure 15 provides a scheme of the architecture of that neural network.

Architecture of CNN includes one convolution layer, one pooling layer, flattened and two fully connected (dense) layers. Convolution layer receives input as a two-dimensional array and converts it to 64 filters with kernel size of 3×3 and valid padding and stride size of 1. Pooling is performed using max operation and pool size of 2×2. Pooling output is then flattened. After that there are two fully connected layers, one of which reduces dimension to 64 using ReLU activation and the other provides reduction to a single continuous output value using sum operation.

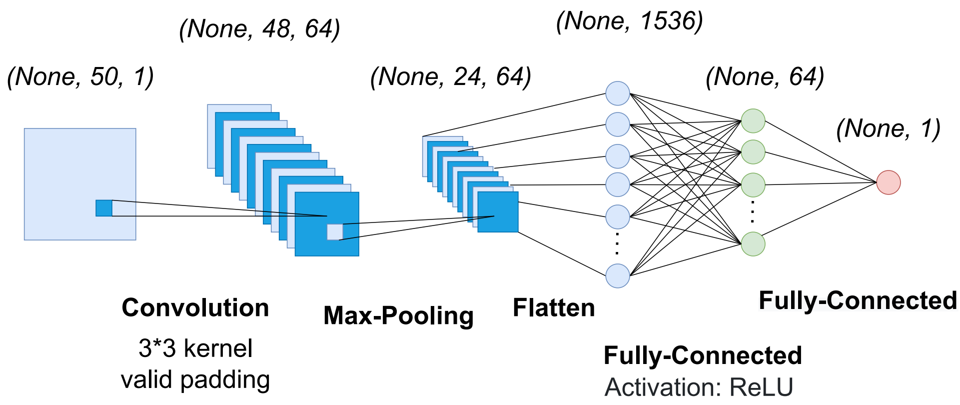

Figure 14. Visualized proposed CNN architecture (adapted from [14,44]).

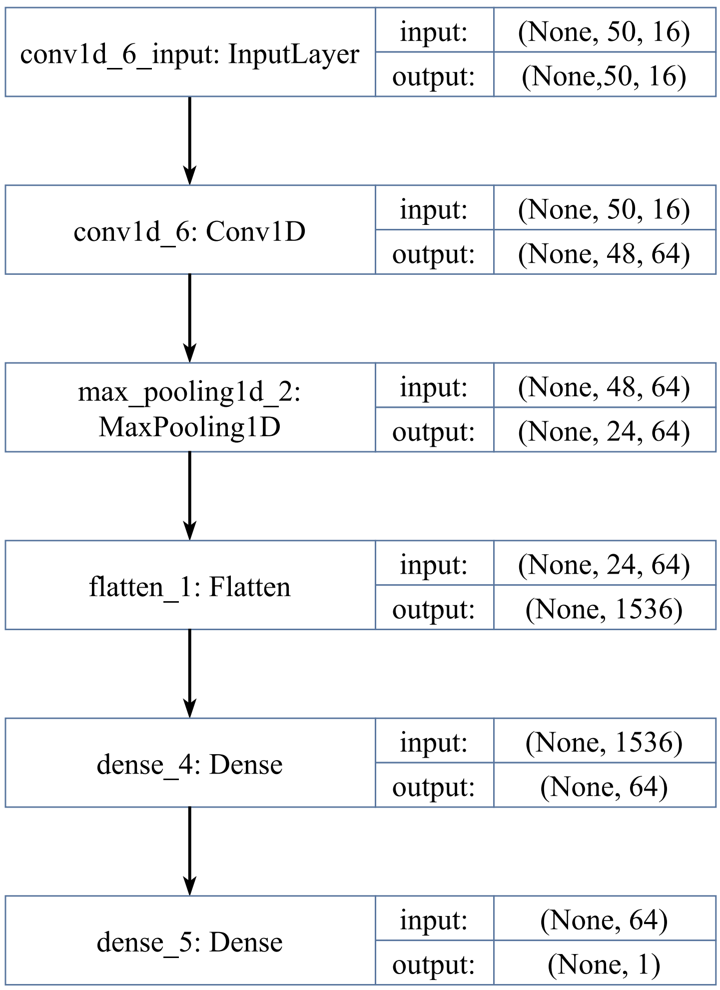

Figure 15. Proposed CNN architecture for RUL forecasting (adapted from [14]).

3. Results

3.1. Datasets

For testing and verification of the proposed DPI method, the simulated data from NASA repository for turbofan engine degradation was used [18]. Data consist of following columns: number of an engine, number of a cycle, 3 input parameters and 21 readings from sensors. In total, there are historical data for 100 engines, each of which has different number of cycles with a total number of 20,631 rows. Figure 16 displays an example of data from the dataset consisting of 10 randomly selected engines.

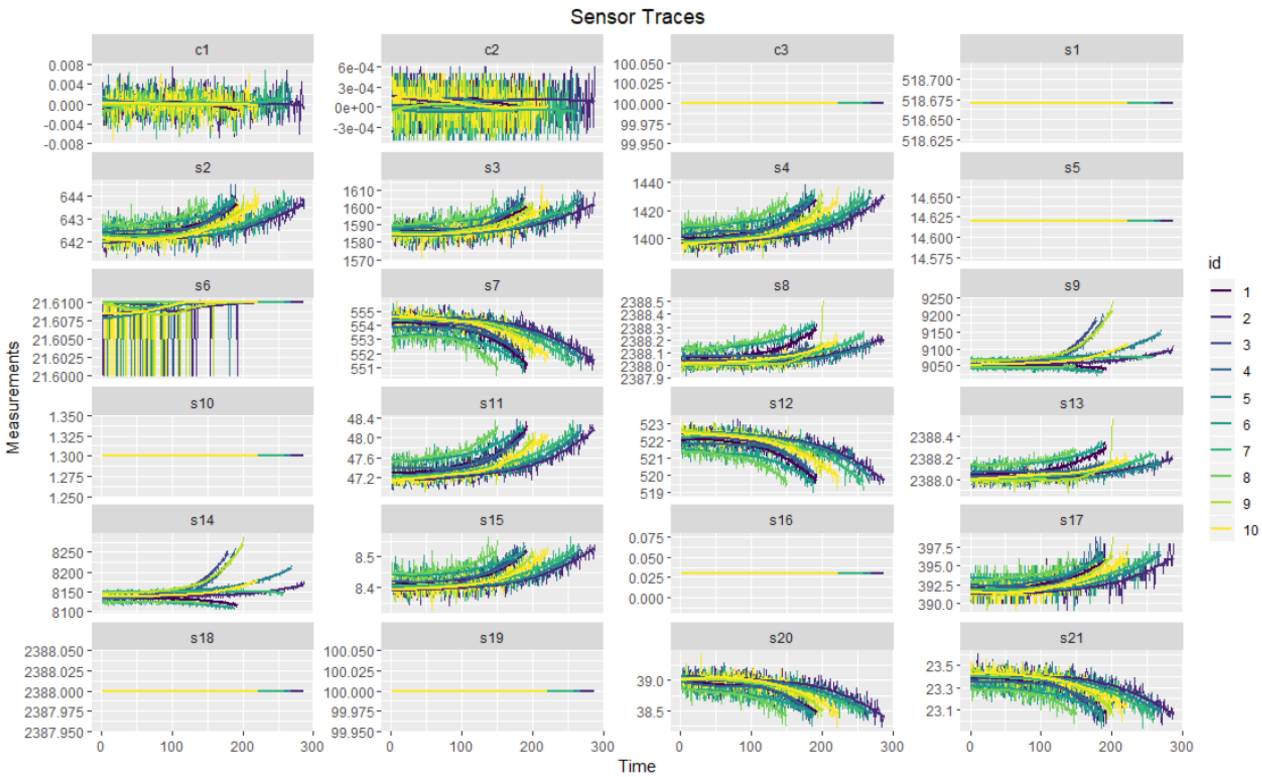

Figure 16. Visualisation of a sample of data from [18].

Table 2 contains parameters of every column in the dataset.

Table 2. Statistical description of test data [18].

Column	Type	Min	Mean	Median	Max
Unit	Numeric	1.000	51.507	52.000	100.000
Time	Numeric	1.000	108.808	104.000	362.000
c1	Numeric	−0.009	0.000	0.000	0.009
c2	Numeric	−0.001	0.000	0.000	0.001
c3	Numeric	100.000	100.000	100.000	100.000
s1	Numeric	518.670	518.670	518.670	518.670
s2	Numeric	641.210	642.681	642.640	644.530
s3	Numeric	1571.040	1590.523	1590.100	1616.910
s4	Numeric	1382.250	1408.934	1408.040	1441.490
s5	Numeric	14.620	14.620	14.620	14.620
s6	Numeric	21.600	21.610	21.610	21.610
s7	Numeric	549.850	553.368	553.440	556.060
s8	Numeric	2387.900	2388.097	2388.090	2388.560
s9	Numeric	9021.730	9065.243	9060.660	9244.590
s10	Numeric	1.300	1.300	1.300	1.300
s11	Numeric	46.850	47.541	47.510	48.530
s12	Numeric	518.680	521.413	521.480	523.380
s13	Numeric	2387.880	2388.096	2388.090	2388.560
s14	Numeric	8099.940	8143.753	8140.540	8293.720
s15	Numeric	8.325	8.442	8.439	8.585
s16	Numeric	0.030	0.030	0.030	0.030
s17	Numeric	388.000	393.211	393.000	400.000
s18	Numeric	2388.000	2388.000	2388.000	2388.000
s19	Numeric	100.000	100.000	100.000	100.000
s20	Numeric	38.140	38.816	38.830	39.430
s21	Numeric	22.894	23.290	23.298	23.618

3.2. Results Description

To improve the accuracy of results, we use the cross-validation technique. Data are split between training and validation sets in proportion of 75%/25%. Further, the training set is split using cross-validation in proportion of 80%/20%, as required by the DPI method.

Results were obtained with open-source Python framework created by authors, which contains an implementation of the proposed method [43].

Example of degradation start points detection is shown at Figure 17.

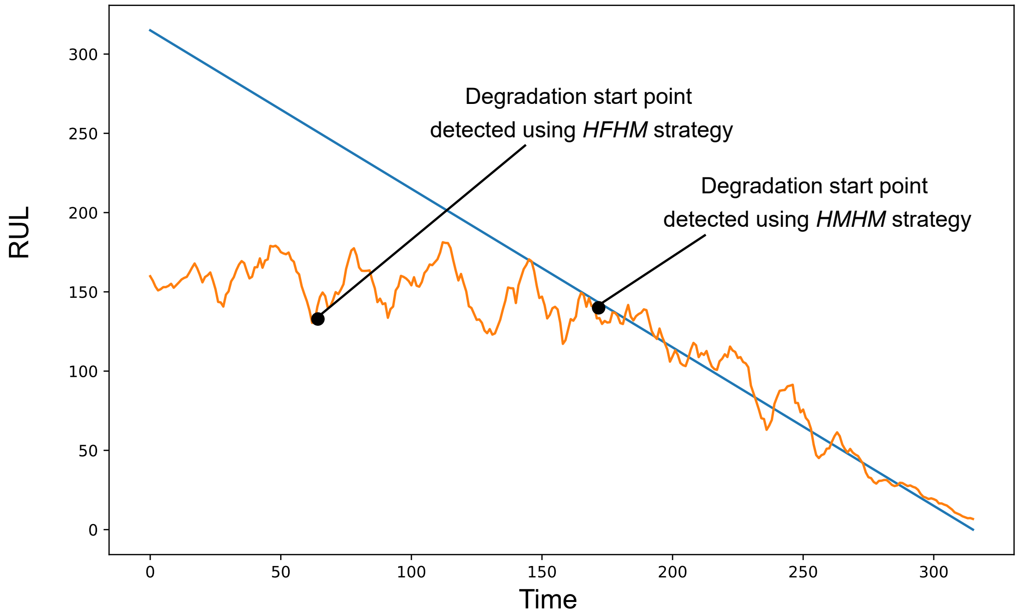

Figure 17. Determination of degradation start point examples. The orange line is an example of RUL forecast obtained using framework [43] for data [18]. The blue line is the expected RUL value.

As can be observed from the given image, the HMHM strategy detects the degradation start point further in the process of operation than HFHM. This can be attributed to the variation in data, e.g., caused by external conditions. The HFHM strategy cannot process this variation, because the original sample is always the same. HMHM strategy can overcome these variations because their longevity is shorter than the "looking back" window of the strategy.

All strategies were tested on the same forecasting model in comparison to the baseline method, which does not include any degradation process detection. The results are provided in Table 3. Strategies that require knowledge of the end of life point are included for reference.

Table 3. Window moving strategies results.

Strategy	MAE Value
CNN (No strategy)	18.35
CNN + HMTF	**4.07**
CNN + HMTM	13.57
CNN + HFTM	15.28
CNN + HFHM	16.12
CNN + HMHM	**9.38**

Each strategy achieves its result by marking different amount of data as degradation process. The percentage of data considered as a degradation process by each of the strategies is provided at Table 4.

Table 4. Window moving strategies results.

Strategy	Degradation Data Percentage
HMTF	5.42
HMTM	51.63
HFTM	87.59
HFHM	90.06
HMHM	43.56

4. Discussion

In the experiment proposed, the DPI method in combination with the forecasting model was compared to the same forecasting model without any additional data preparation conducted as a baseline. The CNN model was selected because of its accuracy and prevalence in recent research. All related to CNN model parameters were kept the same across all tests. Baseline CNN model on the given data with given parameters showed an accuracy of 18.35 points MAE.

The Kruskal-Wallis test helps to determine the start of negative changes in the process we call degradation. The criterion is very basic and effective at the same time, showing the applicability of statistical tests to the data during the degradation start point detection. However, future work may be carried out to devise more comprehensive test for improved accuracy.

Some strategies require additional logic for the degradation start point detection, e.g., HMHM and its lag of a second order l_2, but their primary objective is to make the DPI method less susceptible to random changes in data.

The strategy of moving sliding windows across data is the main variable point in the proposed DPI method. Depending on a strategy, the obtained results vary significantly, which can be attributed to the nature of a specific strategy.

HMTF strategy combined with a baseline CNN forecasting method shows an accuracy of 4.07 MAE, which is, basically, the most accurate result of the proposed method. However it is not applicable to real world scenarios because of: (1) it is required to know when failure is going to happen for this strategy to function; hence, its only a synthetic test of possible capabilities of the proposed method, (2) due to how late in the life of energy equipment it sets a degradation start point, indicated by how little data it considers to be a degradation (only about 5 percent), it would have poor performance in earlier stages of the equipment's life and, thus, late reaction times.

The HMTM strategy shows a result of 13.57 MAE, which is an average result among tested strategies. If we look at the data distribution, we can observe that this strategy finds about 50 percent of data to belong to degradation process. Basically, it means that it puts the degradation start point in the middle of the life of energy equipment most of the times. This can be explained by the nature of the movement of windows in this strategy. They move towards each other with fixed equal speed and meet roughly in the middle. To mitigate this, further improvement to the comparison of data in the windows technique can be conducted. Moreover, it is possible to add a more comprehensive algorithm to adjust the size of a step for each window individually. This strategy is also unusable in the real world scenario because it requires one to know when failure is going to occur.

HFTM shows an accuracy of 15.28 MAE, which is one of the smallest increases in comparison to the benchmark method out of all the strategies. This is because it detects the beginning of the degradation point very early, as can be observed from the fact that part of the data considered that the degradation is over 85 percent. This is contrary to the proposal of splitting the data set into a normal operation and degradation process, as it only takes out small percentage of data. This also is not a very accurate representation of a real world process, as significant degradation would not occur in energy equipment for a majority of its lifespan. Moreover, it means that data that represent a normal operation are going to get mixed with one of the degradation process and decrease the accuracy of the forecasting model. This can be attributed to the first window being fixed, thus giving only a small range of the possible variation of values during the normal operation. The further tuning of sensitivity and the increasing range of the allowed values can be beneficial for the accuracy of this strategy, as it could allow to put the degradation start point further in the lifetime of the energy equipment. This strategy is also not usable in real world scenarios due to the requirement of knowing the end of life.

The HFHM strategy is very similar to a HFTM with 16.12 MAE, but conducted in reverse. it shows that practically the same accuracy and similar percent of data is considered degradation. This strategy, however, can be used in a real world scenario, because it does not require knowledge of the end of life point to function.

Finally, the HMHM strategy that shows the result of 9.38 MAE, which is better than the average but still not as good as HMTF. This strategy considers about 43 percent of data on average to be degradation, which means that it can provide a better reaction time, making the forecast of the remaining useful life when over a third of a lifespan of energy equipment is still left. This strategy is more robust than HFHM because it can account for smaller changes in values from sensors and overall is the most balanced option out of all the considered strategies. A minimum amount of change in the health index, which is required for it to trigger, is higher than in some other strategies, which is going to prevent data from the early stages of operation to mix in with degradation data, while not being too high and having a late reaction time. Moreover, this strategy can be used in a real world scenario because it does not require the coordinate of the end of life to function.

There is an observable correlation between the accuracy of the forecast and position of the degradation start point in the lifespan of the energy equipment. The further the point is, the more accurate the forecast is. This observation supports the trend that the degradation of energy equipment speeds up towards the end of life.

With the use of the proposed degradation start point detection method, it is possible to double the accuracy of the forecasting method in real world scenarios (HMHM strategy) and up to four times increase in the accuracy when performing synthetic tests (HMTF strategy).

Increasing the accuracy of RUL forecast provides higher quality data for the decision support step and allows for increased precision in managerial decisions for maintenance planning. This, in turn, would improve the reaction to possible failures by reducing the chance of failure occurring and reduce operating costs.

We may point to the following limitations of the proposed method:

(1) The method is used on aggregated data for each operation cycle, i.e., each equipment parameter has only one value for each given operation cycle. In real life, we have a set of values for every equipment parameter that describes the operation cycle. The length of the set is defined by the duration of the cycle and granularity of data acquisition. Therefore, we need preprocessed aggregated data to use with the proposed method, which necessitates the additional dependency on data aggregation algorithms.
(2) Tail-based strategies (HMTF, HMTM and HFTM) could not be used in a real life scenario because they require knowledge of the end of life time of equipment to operate; hence, they can only be used as a benchmark on historical data. That is why all our significant results are obtained based on Head-move strategies.
(3) We use aggregated value of RUL forecast based on all parameters to perform DPI, which is a possible limiting factor for achieving the maximum accuracy of the degradation process identification. Thus, a shift to the estimation of the beginning of the degradation process based on individual parameters of equipment and their correlation may give better accuracy and more control over DPI.

5. Conclusions and Future Work

The RUL estimation problem for reliability-centered maintenance energy equipment is considered in this paper. The main contribution of the paper is the unsupervised method for the degradation process identification based on two sliding windows and Kruskal-Wallis test to compare the statistics of data within these windows. Five different strategies of the DPI method were discussed, and the Head Move—Head Move strategy is chosen as more applicable for RUL prediction implementation. Combination of the proposed method for degradation process identification and the state-of-the-art deep neural network approached for RUL estimation allows to decrease forecasting error up to 2 times.

There are three directions of future work for the proposed method:

(1) Implementation of operation cycle data aggregation methods that would improve the accuracy of the degradation process identification. This is important, as the method uses aggregated operation cycle data as input and it might not be readily available in certain use-cases.

(2) Shift to degradation process identification based on an individual detection for each of the parameters of energy equipment instead of using an aggregated value for all parameters. This may give more control over degradation identification process and improve the accuracy of detection, since each parameter might have a different dynamic of degradation.

(3) To support the maintenance of energy equipment at all stages of life cycle in terms of performance and costs, it is necessary to develop approaches for the generation of maintenance actions in time. New and more accurate methods to generate managerial decisions can be created that make use not only of more accurate RUL forecasts, but data about the detected degradation process as well.

Author Contributions: Conceptualization, K.Z. and M.S.; Methodology, K.Z. and M.S.; Software, K.Z.; Validation, K.Z. and M.S.; Investigation, K.Z. and M.S.; Writing—original draft, K.Z. and M.S.; Writing—review & editing, M.S.; Visualization, K.Z.; Supervision, M.S. All authors have read and agreed to the published version of the manuscript.

Funding: This research received no external funding.

Data Availability Statement: Publicly available dataset was analyzed in this study. This data is available at https://www.kaggle.com/datasets/behrad3d/nasa-cmaps.

Conflicts of Interest: The authors declare no conflict of interest.

Abbreviations

The following abbreviations are used in this manuscript:

RUL	Remaining useful life
FM	Forecasting method
DPI	Degradation process identification
DAcq	Data acquisition
DPP	Data pre-processing
DAn	Data analysis
DS	Decision support
MI	Maintenance implementation
Op	Operation
CNN	Convolutional neural network
LSTM	Long short-term memory
DNN	Deep neural network
RNN	Recurrent neural network
MAE	Mean average error
RMSE	Root-mean-square error
HMTF	Head move—Tail fix
HFTM	Head fix—Tail move
HMTM	Head move—Tail move
HFHM	Head fix—Head move
HMHM	Head move—Head move

References

1. Farhat, H.; Salvini, A. Novel Gas Turbine Challenges to Support the Clean Energy Transition. *Energies* **2022**, *15*, 5474. [CrossRef]
2. Manasis, C.; Assimakis, N.; Vikias, V.; Ktena, A.; Stamatelos, T. Power Generation Prediction of an Open Cycle Gas Turbine Using Kalman Filter. *Energies* **2020**, *13*, 6692. [CrossRef]
3. Xu, J.; Wang, Y.; Xu, L. PHM-oriented integrated fusion prognostics for aircraft engines based on sensor data. *IEEE Sens. J.* **2014**, *14*, 1124–1132. [CrossRef]
4. Heng, A.; Zhang, S.; Tan, A.C.; Mathew, J. Rotating machinery prognostics: State of the art, challenges and opportunities. *IEEE Sens. J.* **2014**, *14*, 1124–1132. [CrossRef]
5. Yin, S.; Li, X.; Gao, H.; Kaynak, O. Data-based techniques focused on modern industry: An overview. *IEEE Trans. Ind. Electron.* **2015**, *62*, 657–667. [CrossRef]
6. Antonenko, I.N.; Kryukov, I.E. Information systems and practices of maintenance and repair: Stages of development. *Automation* **2011**, *1*, 37–44.
7. Chen, X.; Yan, R.; Liu, Y. Wind turbine condition monitoring and fault diagnosis in China. *IEEE Instrum. Meas. Mag.* **2016**, *19*, 22–28. [CrossRef]
8. Ahsan, S.; Lemma, T.A. Remaining Useful Life Prediction of Gas Turbine Engine using Autoregressive Model. In Proceedings of the UTP-UMP Symposium on Energy Systems 2017, Perak, Malaysia, 26–27 September 2017.
9. Susto, G.A.; Schirru, A.; Pampuri, S.; McLoone, S.; Beghi, A. Machine learning for predictive maintenance: A multiple classifier approach. *IEEE Trans. Ind. Inform.* **2014**, *11*, 812–820. [CrossRef]
10. Azhmukhamedov, I.M.; Gostyunin, Y.A. Choosing a strategy for maintenance and repair of communication network equipment at oil and gas enterprises. *Eng. Bull. Don* **2017**, *45*, 1–10.
11. Reshetnikov, S.O.; Ivanov, S.L. Integral criterion for assessing the condition of an oil refinery equipment for the Conscientious Maintenance and Repair (CM&R) service system. In Proceedings of the Modern Science: Problems and Ways to Solve them, Kemerovo, Russia, 10–11 December 2015; pp. 36–39.
12. Viet, N.T.; Kravets, A.G. The New Method for Analyzing Technology Trends of Smart Energy Asset Performance Management. *Energies* **2022**, *15*, 6613. [CrossRef]
13. Xu, L.D.; He, W.; Li, S. Internet of things in industries: A survey. *IEEE Trans. Ind. Electron.* **2014**, *10*, 2233–2243. [CrossRef]
14. Sai, W.K.; Shcherbakov, M.V. Residual resource prediction method based on data processing of multi-object complex systems. *Casp. J. Manag. High Technol.* **2019**, *45*, 33–44.
15. Cachada, A.; Barbosa, J.; Leitno, P. Maintenance 4.0: Intelligent and Predictive Maintenance System Architecture. In Proceedings of the 2018 IEEE 23rd International Conference on Emerging Technologies and Factory Automation (ETFA), Turin, Italy, 4–7 September 2018; pp. 139–146.
16. Wang, K. Intelligent Predictive Maintenance (IPdM) System—Industry 4.0 Scenario. *WIT Trans. Eng. Sci.* **2016**, *113*, 259–268.
17. Li, Z.; Wang, Y.; Wang, K. Intelligent predictive maintenance for fault diagnosis and prognosis in machine centers: Industry 4.0 scenario. *Adv. Manuf.* **2017**, *5*, 377–387. [CrossRef]
18. NASA Turbofan Jet Engine Data Set. Available online: https://www.kaggle.com/datasets/behrad3d/nasa-cmaps (accessed on 21 September 2022).
19. Zhang, L.; Liu, Z.; Luo, D. Review of remaining useful life prediction using support vector machine for engineering assets. In Proceedings of the 2013 International Conference on Quality, Reliability, Risk, Maintenance, and Safety Engineering (QR2MSE), Chengdu, China, 15–18 July 2013; pp. 1793–1799.
20. Lu, C.; Wang, Z.; Qin, W.; Ma, J. Fault diagnosis of rotary machinery components using a stacked denoising autoencoder-based health state. *Signal Process.* **2017**, *130*, 377–388. [CrossRef]
21. Huang, H.Z.; Wang, H.K.; Li, Y.F.; Zhang, L.; Liu, Z. Support vector machine based estimation of remaining useful life: Current research status and future trends. *J. Mech. Sci. Technol.* **2015**, *29*, 151–163. [CrossRef]
22. Nieto, P.G.; Garcia-Gonzalo, E.; Lasheras, F.S.; De Cos Juez, F.J. Hybrid PSO–SVM-based method for forecasting of the remaining useful life for aircraft engines and evaluation of its reliability. *Reliab. Eng. Syst. Saf.* **2015**, 138, 219–231. [CrossRef]
23. Yan, M.; Wang, X.; Wang, B.; Chang, M.; Muhammad, I. Bearing remaining useful life prediction using support vector machine and hybrid degradation tracking model. *ISA Trans.* **2020**, *98*, 471–482. [CrossRef]
24. Praveenkumar, T.; Saimurugan, M.; Krishnakumar, P.; Ramachandran, K.I. Fault diagnosis of automobile gearbox based on machine learning techniques. *Procedia Eng.* **2014**, *97*, 2092–2098. [CrossRef]
25. Dhalmahapatra, K.; Shingade, R.; Mahajan, H.; Verma, A.; Maiti, J. Decision support system for safety improvement: An approach using multiple correspondence analysis, t-SNE algorithm and K-means clustering. *Comput. Ind. Eng.* **2019**, *128*, 277–289. [CrossRef]
26. Ng, S.S.; Xing, Y.; Tsui, K.L. A naive Bayes model for robust remaining useful life prediction of lithium-ion battery. *Appl. Energy* **2014**, *118*, 114–123. [CrossRef]
27. Patil, S.; Patil, A.; Handikherkar, V.; Desai, S.; Phalle, V.M.; Kazi, F.S. Remaining Useful Life (RUL) Prediction of Rolling Element Bearing Using Random Forest and Gradient Boosting Technique. In Proceedings of the ASME 2018 International Mechanical Engineering Congress and Exposition, Pittsburgh, PA, USA, 9–15 November 2018.
28. Deutsch, J.; He, D. Using deep learning-based approach to predict remaining useful life of rotating components. *IEEE Trans. Syst. Man Cybern. Syst.* **2017**, *48*, 11–20. [CrossRef]

29. Khumprom, P.; Yodo, N. A Data-Driven Predictive Prognostic Model for Lithium-ion Batteries based on a Deep Learning Algorithm. *Energies* **2019**, *12*, 660. [CrossRef]
30. Zhao, R.; Wang, J.; Yan, R.; Mao, K. Machine health monitoring with LSTM networks. In Proceedings of the 2016 10th International Conference on Sensing Technology (ICST), Nanjing, China, 11–13 November 2016.
31. Sagheer, A.; Kotb, M. Unsupervised pre-training of a Deep LSTM-based Stacked Autoencoder for Multivariate time Series forecasting problems. *Sci. Rep.* **2019**, *9*, 1–16. [CrossRef] [PubMed]
32. Zhang, Y.; Xin, Y.; Liu, Z.W.; Chi, M.; Ma, G. Health status assessment and remaining useful life prediction of aero-engine based on BiGRU and MMoE. *Reliab. Eng. Syst. Saf.* **2022**, *220*, 108–123. [CrossRef]
33. Zhou, F.; Gao, Y.L.; Wang, J.Y. Early diagnosis and life prediction of slowly varying fault based on deep learning. *J. Shandong Univ.* **2017**, *47*, 30–37.
34. Mao, L.; Xu, J.; Chen, J.; Zhao, J.; Wu, Y.; Yao, F. A LSTM-STW and GS-LM Fusion Method for Lithium-Ion Battery RUL Prediction Based on EEMD. *Energies* **2020**, *13*, 2380. [CrossRef]
35. Long, B.; Li, X.; Gao, X.; Liu, Z. Prognostics Comparison of Lithium-Ion Battery Based on the Shallow and Deep Neural Networks Model. *Energies* **2019**, *12*, 3271. [CrossRef]
36. Babu, G.S.; Zhao, P.; Li, X.L. Deep convolutional neural network based regression approach for estimation of remaining useful life. In Proceedings of the International Conference on Database Systems for Advanced Applications, Dallas, TX, USA, 16–19 April 2016; pp. 214–228.
37. Lee, K.B.; Cheon, S.; Chang, O.K. A Convolutional Neural Network for Fault Classification and Diagnosis in Semiconductor Manufacturing Processes. *IEEE Trans. Semicond. Manuf.* **2017**, *30*, 135–142. [CrossRef]
38. Ren, L.; Sun, Y.; Wang, H. Prediction of bearing remaining useful life with deep convolution neural network. *IEEE Access* **2018**, *6*, 13041–13049. [CrossRef]
39. Zhao, J.; Gao, C.; Tang, T.; Xiao, X.; Luo, M.; Yuan, B. Overview of Equipment Health State Estimation and Remaining Life Prediction Methods. *Machines* **2022**, *10*, 422. [CrossRef]
40. Sai, W.K.; Shcherbakov, M. Forecasting of high frequency time series with machine learning and statistical methods. *Bull. Comput. Inf. Technol.* **2020**, *6*, 3–11.
41. Wang, H.K.; Cheng, Y.; Song, K. Remaining Useful Life Estimation of Aircraft Engines Using a Joint Deep Learning Model Based on TCNN and Transformer. *Comput. Intell. Neurosci.* **2021**, *2021*, 5185938. [CrossRef] [PubMed]
42. Kruskal, W.H.; Wallis, W.A. Use of Ranks in One-Criterion Variance Analysis. *J. Am. Stat. Assoc.* **1952**, *260*, 583–621. [CrossRef]
43. "Dataworks"—Remaining Useful Life Forecasting Framework. Available online: https://github.com/zadiran/dataworks (accessed on 26 December 2022).
44. A Comprehensive Guide to Convolutional Neural Networks. Available online: https://towardsdatascience.com/a-comprehensive-guide-to-convolutional-neural-networks-the-eli5-way-3bd2b1164a53 (accessed on 24 September 2022).